
Fifth International Conference on
Recent Advances in Geotechnical Earthquake Engineering and Soil Dynamics
and Symposium in Honor of Professor I.M. Idriss
May 24-29, 2010 • San Diego, California

SEISMIC SOIL PRESSURES ON RIGID WALLS WITH SLOPED BACKFILLS

Guoxi Wu , Ph.D., P.Eng
BC Hydro
A02 - 6911 Southpoint Drive, Burnaby, BC, CANADA, V3N 4X8

ABSTRACT

Wood (1973) provided analytical solutions for the response of a rigid wall retaining elastic uniform soil backfill of finite length subjected to harmonic base excitation. Wu and Finn (1999) proposed a modified shear beam solution and derived closed-form formulations for computing dynamic soil pressures under harmonic loading. However, for rigid walls retaining sloped backfills, analytical solutions are not available for computing seismic soil pressures against the walls.

In the current study, seismic soil pressures on rigid walls retaining 2H:1V (27°) sloped backfills have been computed using a total of eight acceleration time histories recorded in past large earthquakes. These records were selected and linearly scaled to three levels of ground motions with a nominal PGA of 0.26g, 0.48g and 0.71g. Nonlinear time-history analyses were conducted using the computer program VERSAT-2D which uses a hyperbolic stress – strain model to simulate the hysteresis response of soil under cyclic loads. Soil pressure diagrams are shown in the paper for horizontal backfills (φ=32°), and for sloped backfills with loose sand (φ=32°) and dense sand (φ=40°) under the three levels of ground motions.

A soil pressure coefficient, K_{0E}, has been introduced to represent the total static and seismic pressures on a rigid (or non-yielding) wall. It is found that K_{0E} varies from 1.1, 1.7 to 2.2 for horizontal backfills under ground motions of 0.26g, 0.48g and 0.71g, respectively. K_{0E} increases to 2.7, 3.8 and 4.9 for the 27° sloped backfills under the same three levels of ground motions, respectively. The point of thrust is at about 0.47H above the base of wall for horizontal backfills, but for sloped backfills it increases to 0.53H for loose sand and 0.55H for dense sand.

INTRODUCTION

Wood (1973) provided analytical solutions for the response of a rigid wall retaining elastic uniform soil backfill of finite length subjected to harmonic base excitation. Due to its mathematical complexity, the application of Wood's solution is very much limited to a very low vibration frequency or the so-called static solution. Wu and Finn (1999) proposed a modified shear beam solution and derived closed-form formulations for computing dynamic soil pressures under harmonic loading. For earthquake loading, they provided design charts of seismic soil pressures that take into account the effect of vibration frequency on the thrust. However, these solutions are only applicable for horizontal backfills.

For rigid walls retaining sloped backfills, analytical solutions are not available for computing seismic soil pressures against the walls.

In the present study, dynamic finite element time-history analyses have been conducted for solving the problem. The numerical procedure, using a commercially available computer program VERSAT-2D (Wutec Geotechnical International 2001), employs a nonlinear hyperbolic stress – strain model to simulate the hysteresis response of soil under cyclic loads. The nonlinear model accounts for soil stress failure and permanent plastic deformations under seismic loads. The method is first verified by comparing its results for rigid walls retaining horizontal backfills with those by Wood (1973) and Wu and Finn (1999). The procedure is then extended to computing soil pressures for rigid walls retaining 2H:1V sloped backfills, i.e., a slope angle of 26.6°. The study examined soil pressures for loose backfills with φ=32° and for dense backfills with φ=40° under three levels of ground motions with a nominal PGA of 0.26g, 0.48g and 0.71g.

INPUT GROUND MOTIONS

For a seismic upgrade project for BC Hydro's Ruskin dam, located at about 8 km northwest of Mission, B.C., dynamic finite element analyses were conducted to assess the seismic soil pressures against a concrete wing wall of a spillway channel. In the process, eight acceleration time histories recorded from past large earthquake were selected. The use of natural records in a dynamic time-history analysis has the advantage in preserving the characteristics of ground motions recorded from real earthquakes (Boomer and Acevedo 2004).

Uniform hazard response spectra (UHRS) for the Ruskin rock site were developed by BC Hydro for earthquakes with annual exceedance frequency (AEF) of 1/10,000, 1/2475, and 1/475. The peak ground accelerations (PGA) of ground motions corresponding to the three levels are 0.71g, 0.48g and 0.26g, respectively.

In current study, natural ground motion records are selected and scaled individually to generally match the 1/2475 UHRS for periods of 0 to 2 seconds. The following criteria were used in the search of acceleration time histories recorded from past large earthquakes:

- Crustal earthquakes with magnitude ranging from M=6.3 to 7.6 and closest distance to fault rupture from 0 to 15 km
- Earthquake source mechanism including strike slip, reverse normal and reverse-oblique, but not including normal or normal-oblique due to local tectonic setting
- A bedrock site or a stiff soil site with a minimum average shear wave velocity of 560 m/s for the upper 30 m (V_{s30}).
- The acceleration response spectrum of a record after being scaled linearly shall closely match the 1/2475 UHRS.

The record search was carried out primarily from the PEER NGA and the COSMOS record databanks. The Pacific Earthquake Engineering Research Center maintains the PEER NGA databank which can be found in http://peer.berkeley.edu/smcat/. The Consortium of Organization for Strong-Motion Observation Systems (COSMOS) manages the COSMOS virtual data centre that can be located in http://db.cosmos-eq.org/scripts/default.plx. The core members of COSMOS include US Geological Survey, California Geological Survey, US Army Corps of Engineers and US Bureau of Reclamation.

Due to insufficient number of earthquake records that satisfy all selection criteria, some selection requirements were relaxed to include ground motions recorded at an earthquake source-site distance of 30 km and site shear wave velocity less than 560 m/s.

A total of eight earthquake records were selected from this process. These records consists of ground motions recorded from seven past earthquakes with a magnitude ranging from M=6.3 to 7.6. Relevant parameters of the eight records are shown in Table 1 which includes magnitude, mechanism, source-site distance, site condition as well as the recorded peak ground acceleration (PGA), peak ground velocity (PGV) and peak ground displacement (PGD) of each component of the three dimensional ground motion arrays.

The scaling factors applied to the recorded ground motions to match the 1/2475 UHRS are also shown in Table 1. Only one horizontal component for each of the eight records was used in the current study of seismic soil pressure. Response spectra of the eight horizontal acceleration records, after scaling, are plotted in Fig. 1. An average response spectrum of the eight spectra is obtained and compared in Fig. 2 with the 1/2475 UHRS for the Ruskin site and for a NBCC 2005 Class C soil site in Vancouver (Adams and Atkinson 2003).

It is seen that an individual record always results in response higher at one period and lower at another period than the target values. The average response of the selected eight records reasonably represents the target response over a period range of 0.1 to 2.0 sec.

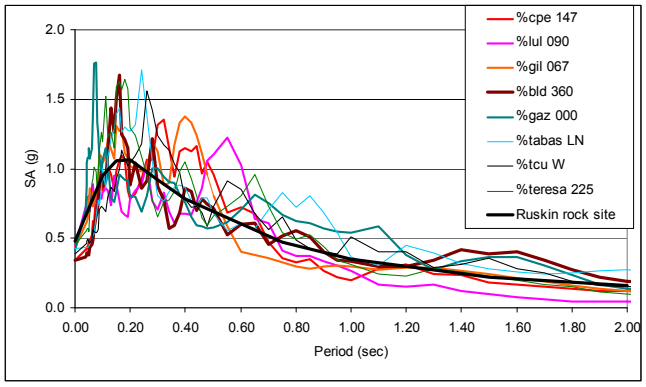

Fig. 1. Response spectrum of the eight records after scaling for ground motions with AEF of 1/2475

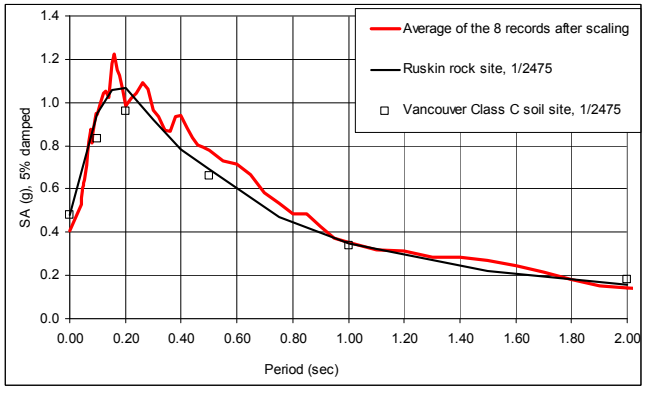

Fig. 2. A comparison of the average response spectrum of the eight records and the uniform hazard response spectra

Table 1. Summary of the Eight Earthquake Records for Ground Motions with AEF of 1/2475

Record #	Earthquake, Station & Short Name	Magnitude	Mechanism	Duration (sec)	R_{RUP} (km)	R_{JB} (km) [1]	V_{s30} (m/s)	Geomatrix Class	Component [2]	PGA [3] (g)	PGV [3] (cm/s)	PGD [3] (cm)	Scaling Factor	PGA after scaling (g)
1	1989/10/18 US Loma Prieta, Santa Teresa Hills San Jose, %teresa	6.9	Reverse Oblique	50	15	14	672	A	**#225 (S)**	**0.274**	**26.2**	**13.15**	**1.6**	**0.438**
									#315	0.228	20.6	5.27	1.6	0.365
									Up/Down	0.209	16.7	4.97	1.6	0.334
2	1999/09/20 Taiwan Chi-Chi, TCU071, %tcu	7.6	Reverse Normal	90	5	0	625	A	N	0.655	69.4	49.06	0.7	0.459
									W (S)	**0.567**	**44.4**	**13.76**	**0.7**	**0.397**
									V	0.449	34.8	31.32	0.7	0.314
3	1978/09/16 Iran Tabas, 9101 Tabas, %tabas	7.4	Reverse Normal	33	2	2	767	A	**LN (S)**	**0.836**	**97.8**	**36.92**	**0.5**	**0.418**
									TR	0.852	121.4	94.58	0.5	0.426
									UP	0.688	45.6	17.04	0.5	0.344
4	1976/05/17 USSR Gazli, 9201 Karakyr, %gaz	6.8	Reverse Normal	16	5	4	660	A	**#000 (S)**	**0.608**	**65.4**	**25.29**	**0.7**	**0.43**
									#090	0.718	71.6	23.71	0.7	0.50
									Up/down	1.264	64.2	30.15	0.35	0.44
5	1994/01/17 US Northridge, #24157 Baldwin Hills LA, %bld	6.7	Reverse Normal	40	30	23	297	B	#090	0.239	14.9	6.17	2.0	0.48
									#360 (S)	**0.168**	**17.6**	**4.79**	**2.0**	**0.34**
									Up/down	0.091	8.4	3.29	2.0	0.18
6	1989/10/18 US Loma Prieta, 47006 Gilroy Gavilan College, %gil	6.9	Reverse Oblique	40	10	9	730	B	**#067 (S)**	**0.357**	**28.6**	**6.35**	**1.2**	**0.43**
									#337	0.325	22.3	4.59	1.2	0.39
									Up/down	0.191	12	5.77	1.2	0.23
7	1980/05/25 US Mammoth Lakes, 54214 Long Valley dam (Upr L Abut), %lul	6.3	Reverse Oblique	30	15	13	345	A	#000	0.43	23.6	7.52	1.6	0.69
									#090 (S)	**0.271**	**13.9**	**3.06**	**1.6**	**0.43**
									Up/Down	0.123	8.4	1.72	1.6	0.20
8	1979/10/15 US Imperial Valley, 6604 Cerro Prieto, %cpe	6.5	Strike Slip	64	15	15	660	A	**#147 (S)**	**0.169**	**11.6**	**4.25**	**2.0**	**0.34**
									#237	0.157	18.6	7.95	2.0	0.31
									Up/Down	0.212	6.8	3.29	2.0	0.42

[1] R_{RUP} = Closest distance to rupture plane; R_{JB} = Closest Horizontal Distance to rupture plane
[2] (S) = horizontal component selected to be used in the dynamic time-history analyses
[3] PGA, PGV, PGD are for original (not scaled) earthquake records

VERSAT-2D BACKGROUND

VERSAT-2D (Wutec Geotechnical International 2001) is a 2-dimensional finite element program that is used to conduct static and dynamic stress and deformation analyses of earth structures subjected to base excitation or to dynamic loads at specified locations (Wu 2001; Wu and Chan 2002; Wu et al. 2006). The program includes a non-linear hyperbolic model to simulate the hysteresis response of soil under cyclic loads. Excess pore water pressures caused by cyclic loads, if applicable, can also be computed. Large ground displacements caused by excess earthquake loading are calculated using the updated Lagrangian analysis. Structural beam elements and bar elements are used for modeling soil-structure interaction.

Earthquake firm-ground accelerations are applied at the base of the model, and displacements relative to the model base are computed. Inertial forces on the soil mass caused by base motions are computed using Newton's law, and base accelerations are used directly in the equations of motions.

The equations of motions describing the incremental dynamic force equilibrium are given as:

$$[M]\{\Delta \frac{d^2\delta}{dt^2}\} + [C]\{\Delta \frac{d\delta}{dt}\} + [K]\{\Delta\delta\} = \{\Delta P\} \quad (1)$$

Where

[M] = mass matrices
[C] = viscous damping matrices
[K] = tangent stiffness matrices
$[\Delta\delta]$ = incremental displacement matrices
$[\Delta d\delta/dt]$ = incremental velocity matrices
$[\Delta d^2\delta/dt^2]$ = incremental acceleration matrices
$[\Delta P]$ = incremental external load matrices.

VERSAT-2D uses the hyperbolic stress - strain model to simulate the nonlinear and hysteresis shear stress - strain relationship for soils (Finn et al., 1977). The low-strain shear modulus, G_{max}, and the bulk modulus, B, are stress level dependent and computed as follows:

$$G_{\max} = K_g P_a (\frac{\sigma_m'}{P_a})^m \quad (2)$$

$$B = K_b P_a (\frac{\sigma_m'}{P_a})^n \quad (3)$$

Where

P_a = atmospheric pressure, 101.3 kPa
K_b = bulk modulus constant
K_g = shear modulus constant
m, n = shear modulus exponential, and bulk modulus exponential, respectively
σ_m' = effective mean normal stress.

The relationship between the shear stress, τ_{xy}, and the shear strain, γ, for the initial loading condition is modelled to be nonlinear and hyperbolic as follows:

$$\tau_{xy} = \frac{G_{\max}\gamma}{1 + G_{\max}/\tau_{ult} \bullet |\gamma|} \quad (4)$$

Where

τ_{ult} = ultimate shear stress in the hyperbolic model
G_{max} = low-strain shear modulus.

Usually τ_{ult} is assumed to be the shear strength of the soil element (Finn et al. 1977). However, in VERSAT-2D, τ_{ult} can also be determined using a modulus reduction factor R_f. By using an appropriate R_f factor the hyperbolic model allows a specified shear modulus reduction curve and damping curve to be matched at the strain range of interest (Wu 2001). A R_f of 1000 has been used for sandy soils in this study.

The Masing criterion has been used to simulate the shear stress-strain relationship during unloading and reloading. The extended application of Masing criterion to irregular loading such as earthquake loading was also presented by Finn et al. (1977).

In addition to the hysteresis response, stresses at each Gauss points in a finite element are checked continuously with time of integration, and corrected when necessary, so that the stresses are consistent with the Mohr-Coulomb failure criterion for soils.

SEISMIC SOIL PRESSURES FROM HORIZONTAL BACKFILLS

A finite element model developed for this analysis is shown in Fig. 3, which consists of a 5 m thick and 80 m long sandy and dry backfill. The backfill is modeled using 3500 soil elements with 25 uniform grids in the vertical direction and 140 non-uniform grids in the horizontal direction. The horizontal grids are sized to be 0.2 m each within 5 m of the wall, 0.5 m each for another 15 m, and 85 grids for remaining 60 m (approximately 0.71 m each). The left side boundary is fixed to the model base for horizontal motion, and horizontal stresses at soil elements adjacent to the left side boundary are recorded as soil pressure against a rigid or non-yielding wall.

Typical soil parameters for loose sand are used for the backfill, including unit weight of γ=19 kN/m^3, zero cohesion and friction angle of φ=32°, shear modulus constant of K_g=868, bulk modulus constant of K_b=2118, and m=0.5 and n=0.5. Dynamic time-history analyses are initiated following a static stress analyses. For horizontal backfill, a static lateral stress coefficient of K_0=0.47 is obtained.

Three levels of ground motions are applied to the model:

- AEF of 1/475 (0.26g): uniformly reducing the scaling factors in Table 1 by 0.54 (=0.26/0.48)
- AEF of 1/2475 (0.48g): using scaling factors in Table 1
- AEF of 1/10,000 (0.71g): uniformly increasing the scaling factors in Table 1 by 1.48 (0.71/0.48).

The above linear scaling assumes that the shapes of the response spectra for the three levels of ground motions are similar. This assumption is considered reasonable after comparing UHRS curves of the three. However, the use of Chi-Chi record (%tcu) as 1/475 ground motion may be too strong for ground displacement prediction. For analysis of seismic soil pressure, it is considered to be acceptable.

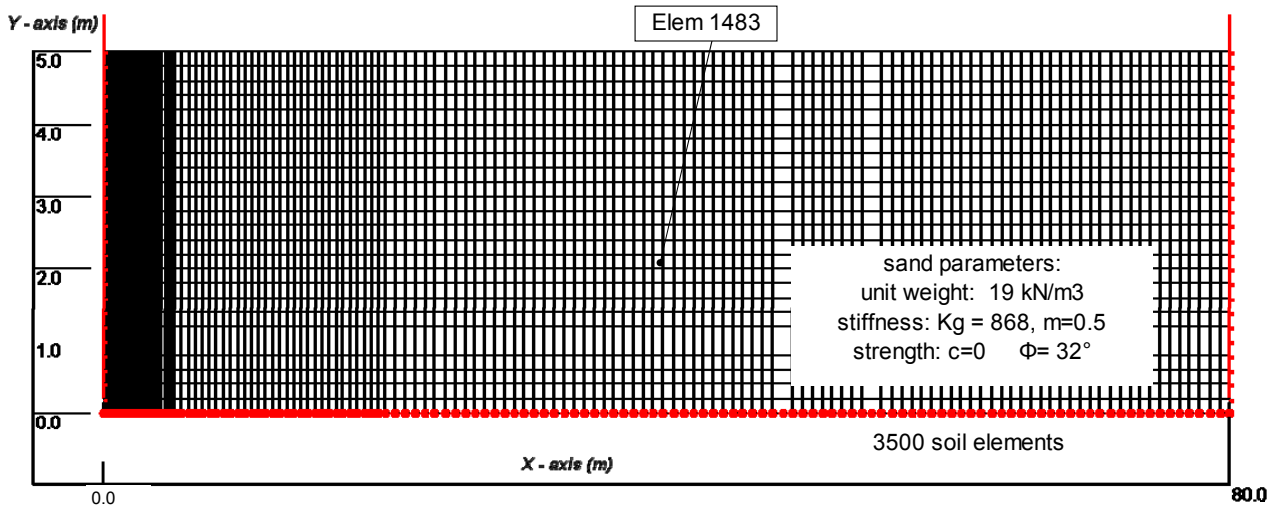

Fig. 3. VERSAT-2D finite element grid and boundary conditions for a 5 m high wall and horizontal backfills

The nonlinear and hysteretic response of soil under cyclic loading, as simulated in VERSAT-2D, is shown in Fig. 4 for Element 1483 (see Fig. 3 for its location) using the record 1/2475:%gaz. From 0 to 5.5 sec the shaking level is low with shear strain less than 0.03%, thus the shear stress and strain response is stiff with low hysteretic damping. During strong shaking from 5.5 to 6.5 sec, shear strain increases to 0.15% and the hysteretic damping increases to about 18%.

The first mode frequency of the wall-soil system also shows significant reduction at the time of strong shaking (Fig. 5) because the stiffness of the soil decreases at larger strains.

Time histories of horizontal stresses for 4 of the 25 soil elements adjacent to the left side boundary (the wall) are shown in Fig. 6. Soil pressures increase significantly at the time of strong shaking after 5.5 sec. It is noted that soil pressures at various depths along the wall are in phase. Maximum total soil pressures, including static soil pressure, are about 79 kPa, 92 kPa, 87 kPa, 71 kPa at depths of 1.1 m, 2.1 m, 3.1 m and 4.1 m, respectively.

Maximum total soil pressures versus depth are shown in Figs. 7, 8 and 9 for ground motions of 0.26g, 0.48g and 0.71g, respectively.

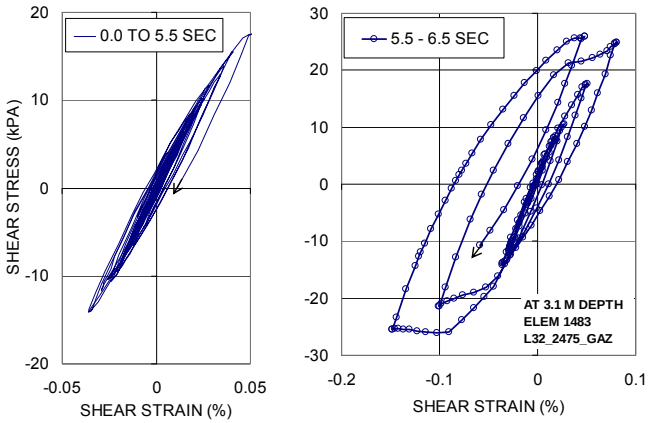

Fig. 4. Hysteretic shear stress and strain traces at Element 1483 from 0 to 6.5 sec (1/2475: record %gaz)

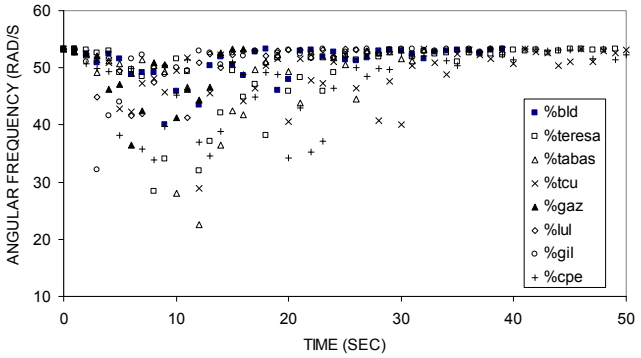

Fig. 5. Time histories of the 1st mode angular frequency of the wall-soil system for ground motions with AEF of 1/2475

The total force on the wall from soil pressure is defined as

$$P_{0E} = \tfrac{1}{2} K_{0E} \gamma H^2 \qquad (5)$$

where K_{0E} is a soil pressure coefficient proposed for rigid wall, γ is soil unit weight, and H is wall height. K_{0E} includes both static and seismic soil pressures.

For ground motions of 0.26g (1/475), values of K_{0E} vary in a narrow range from 1.0 for %gaz to 1.21 for %tabas. For ground motions of 0.48g (1/2475), values of K_{0E} are in the range of 1.5 to 1.8 among the eight input records. For ground motions of 0.71g (1/10,000), values of K_{0E} increase to 1.9 for %cpe and 2.4 for %teresa.

Average values of K_{0E} from the eight input records are 1.1, 1.7 and 2.2 for ground motions of 0.26g, 0.48g and 0.71g, respectively.

Results of VERSAT-2D nonlinear dynamic analyses are compared well in Fig. 10 with those of Wood (1973) and Wu and Finn (1999). K_{0E} for Wood (1973) is calculated from static K_0 plus two times K_h for seismic component, and K_h of 0.26, 0.48 and 0.71 are used. K_{0E} for Wu and Finn (1999) is estimated using the curves for a parabolic modulus profile. As expected, K_{0E} from VERSAT-2D nonlinear dynamic analysis agrees well with the upper values of Wu and Finn (1999) at a frequency ratio of 0.7 – 1.0.

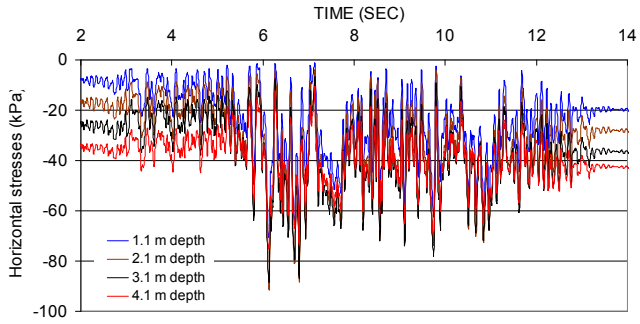

Fig. 6. Time histories of soil pressures at selected locations of the wall from 2 to 14 sec (1/2475: record %gaz)

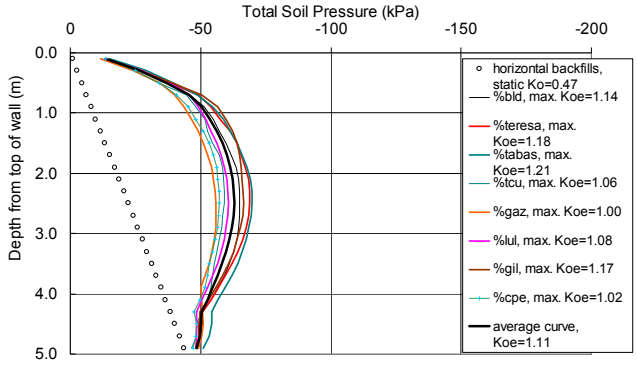

Fig. 7. Maximum soil pressures for ground motions with AEF of 1/475 (0.26g)

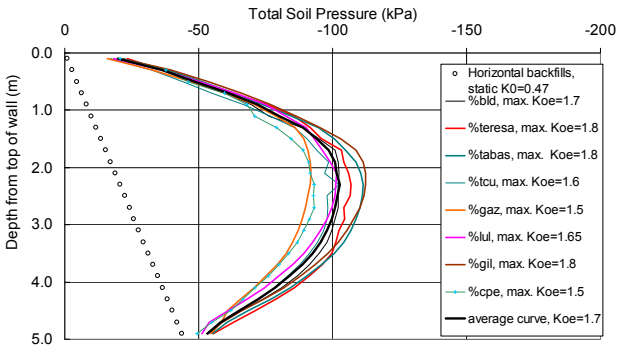

Fig. 8. Maximum soil pressures for ground motions with AEF of 1/2475 (0.48g)

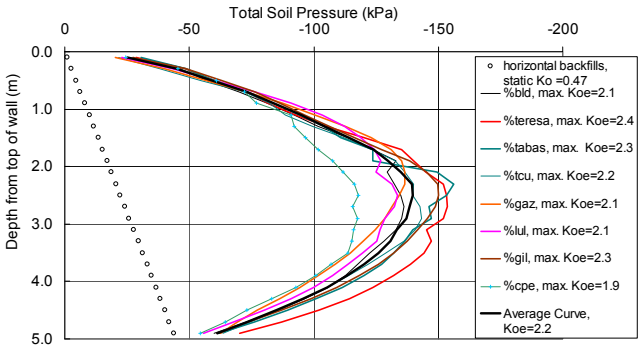

Fig. 9. Maximum soil pressures for ground motions with AEF of 1/10,000 (0.71g)

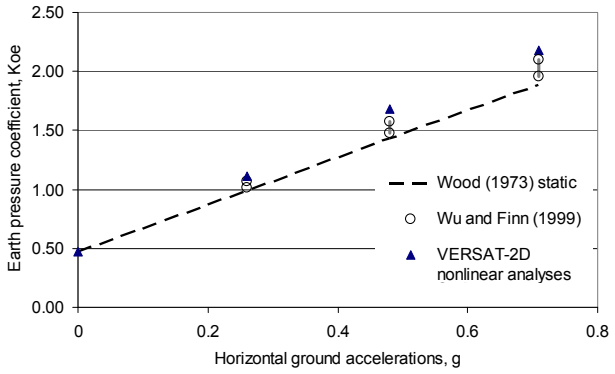

Fig. 10. K_{OE} from VERSAT-2D nonlinear analyses, Wood (1973) and Wu and Finn (1999) for horizontal backfills

SEISMIC SOIL PRESSURES FROM SLOPED BACKFILLS

The analyses were carried out also for a 5 m high wall, but the wall retains 2H:1V sloped backfills. Two scenarios on backfills were examined in this study:

- Case 1: Backfill is comprised of loose sand, i.e., the same as that for the horizontal backfill (γ=19 kN/m^3, φ=32°, Kg=868 and others)
- Case 2: Backfill is comprised of dense sand with γ=20.5 kN/m^3, φ=40° and Kg=1736

The finite element model is same for Case 1 and Case 2, and it consists of 7487 soil elements. The left side boundary is fixed to the model base in both vertical and horizontal motions, while the right side boundary is free in vertical motion. The slope is 25 m high, and the slope crest is 50 m from the top of the wall (Fig. 11).

Ground Displacements

A key feature of a rigid wall retaining sloped backfills is that a large amount of soils is vulnerable to yielding subject to severe earthquake loading. While soils on slope tend to yield in shearing, soils behind the wall would yield in passive. Thus stresses of soils behind the upper part of the wall are limited by passive soil pressures. Stresses in the lower portion of the backfill are less or not affected by strength failure of soils.

Slope deformations caused by soil yielding are illustrated in Fig. 11 for the loose sand backfill subject to the record 1/10,000:%cpe. At the end of ground shaking, the computed ground displacements at the slope crest are 2.5 m laterally and 1.6 m downward. The pattern of deformation is shown by the distorted grids, compared to the straight reference line prior to ground shaking.

Yield acceleration of the soil slope is also captured by the finite element time-history analysis. Acceleration response at the slope crest is shown in Fig. 12 for illustration. It is seen that the acceleration response in the down-slope direction (positive sign) is very much capped by the yield acceleration of the soil slope, probably in the order of 0.2g or less. Permanent ground displacement is induced as ground accelerations exceed the yield acceleration, as shown also in Fig. 12.

Ground displacements computed from VERSAT-2D nonlinear dynamic analyses are summarized in Table 2 for the loose and dense sand slopes subject to the three levels of ground shaking. Results from a total of 48 time-history analyses are presented. Lateral displacements (average) in the order of 1.9 m, 1.1 m and 0.4 m are predicted to occur at the crest of the loose sand slope under ground motions with AEF of 1/10,000, 1/2475 and 1/475, respectively. The lateral displacements (average) are expected to decrease to the order of 0.66 m, 0.26 m and 0.05 m for a dense sand slope under the three levels of ground motions, respectively.

Seismic Soil Pressure for Loose Sand Backfill

Seismic soil pressures determined from the analyses are plotted in Figs. 13 to 15 for loose sand backfills. Static soil pressures on the wall increase from K_0=0.47 for a horizontal backfill to K_0=1.5 for the 27° sloped backfill.

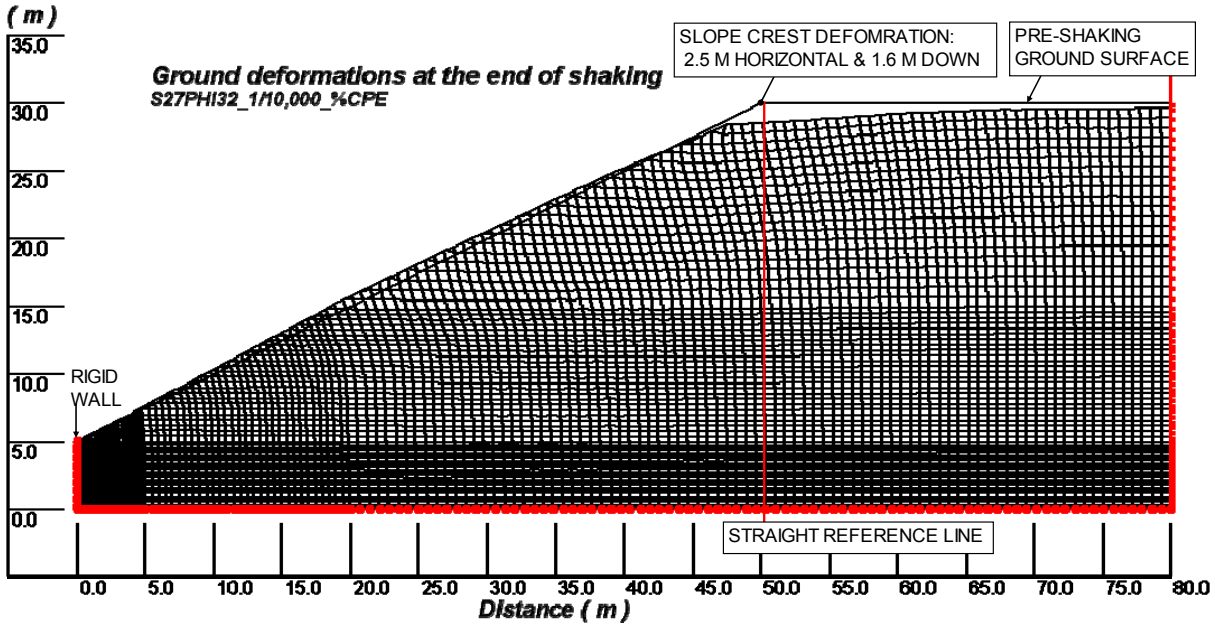

Fig. 11. Deformed 2H:1V sloped soil backfill (φ=32°) (1/10,000: record %CPE)

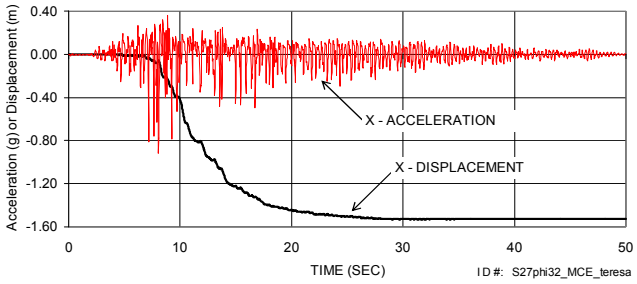

Fig. 12. Time history of accelerations and displacements at the slope crest (1/10,000: record %teresa)

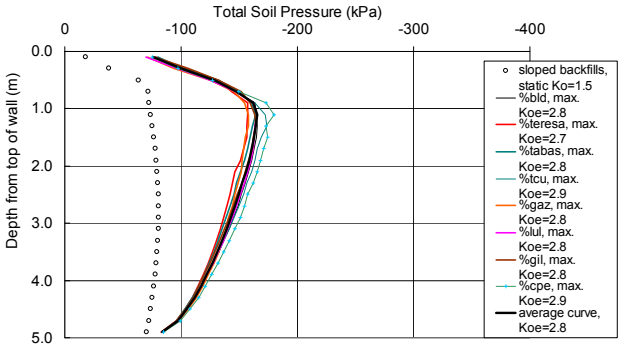

Fig. 13. Maximum soil pressures on walls with 2H:1V sloped backfills (φ=32°) under 1/475 ground motions

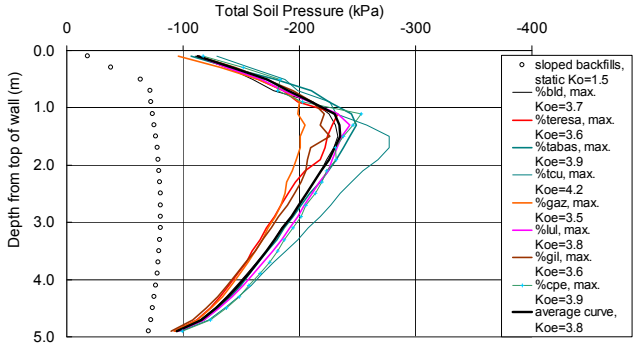

Fig. 14. Maximum soil pressures on walls with 2H:1V sloped backfills (φ=32°) under 1/2475 ground motions

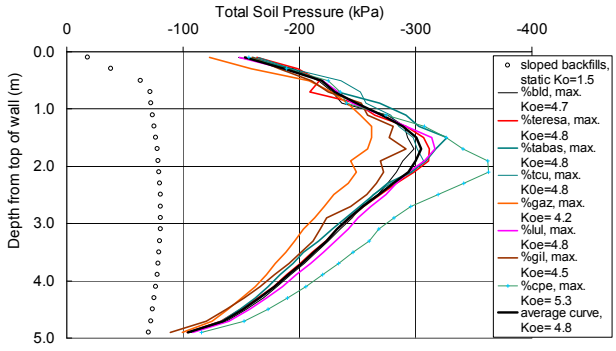

Fig. 15. Maximum soil pressures on walls with 2H:1V sloped backfills (φ=32°) under 1/10,000 ground motions

For the 1/475 ground motions, maximum seismic thrusts on the wall fall in a narrow band among the eight individual input records. K_{0E} varies slightly from 2.7 for %teresa to 2.9 for %tcu and %cpe. For the 1/2475 ground motions, the record %tcu results in higher seismic pressures (K_{0E}=4.2) than the rest of the eight records (K_{0E}=3.5 to 3.9). For the 1/10,000 ground motions, the record %cpe results in the highest pressures with K_{0E} of 5.3, while K_{0E} from the remaining records varies from 4.5 to 4.8.

K_{0E} for the average curves are 2.8, 3.8 and 4.8 for ground motions with 0.26g, 0.48 g and 0.71g, respectively.

It is noted that seismic pressures due to the record %cpe are lowest for horizontal backfills, but they become the highest for the sloped backfills. In contrast, the record %gil tends to yield highest soil pressures for horizontal backfill, but it results in the 2nd lowest soil pressures for the sloped backfills. These are result of interaction between the soil-wall model, characteristics of input motions, as well as nonlinear response of soil. These results demonstrate the necessity of using a basket of ground motions, as compared to a single input record, in dynamic time-history analyses.

The analyses reveal two distinct features of seismic soil pressures for sloped backfills, as compared to horizontal backfills. First, the resultant force (thrust) acts higher above the base of wall. For ground motions with AEF of 1/475, 1/2475 and 1/10,000, the points of thrusts from the average curves are located at 0.52H, 0.53H and 0.54H above the base of wall, respectively. For horizontal backfills, they are at 0.47H, 0.48H, and 0.48H for the three levels of ground motions, respectively. Secondly, dynamic soil pressures close to the top of wall appear to be constrained by passive failure of soils. The results also indicate that the passive failure zone becomes deeper as the level of shaking increases from 0.26g to 0.71g.

Seismic Soil Pressures for Dense Sand Backfill

Seismic soil pressures for dense sand backfills (φ=40°) are shown in Figs. 16 to 18.

In general, seismic soil pressures from dense backfills act higher above the base of wall than those from loose backfills. The points of thrusts from the average curves are located at 0.54H, 0.55H and 0.56H above the base of wall for ground motions with AEF of 1/475, 1/2475 and 1/10,000, respectively. This is because depth of passive failure zone decreases in dense sand due to its higher shear strength than loose sand.

For the 1/475 ground motions, variation of maximum seismic pressure profiles among the eight input records is quite small. K_{0E} varies slightly from 2.4 for %lul to 2.8 for %gil and %cpe. For the 1/2475 ground motions, the record %lul yields lowest seismic pressures with a K_{0E} of 3.4, while the record %gil results in the highest pressures with a K_{0E} of 4.3. The remaining K_{0E} falls in the range of 3.7 to 4.0. For the 1/10,000 ground motions, the record %gil again results in the highest pressures with a K_{0E} of 5.3, while K_{0E} from the remaining records varies from 4.6 to 5.1.

K_{0E} for the average curves are 2.6, 3.8 and 5.0 for ground motions with 0.26g, 0.48 g and 0.71g, respectively.

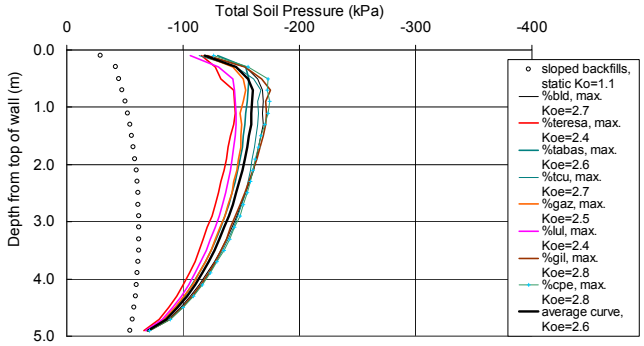

Fig. 16. Maximum soil pressures on walls with 2H:1V sloped backfills (φ=40°) under 1/475 ground motions

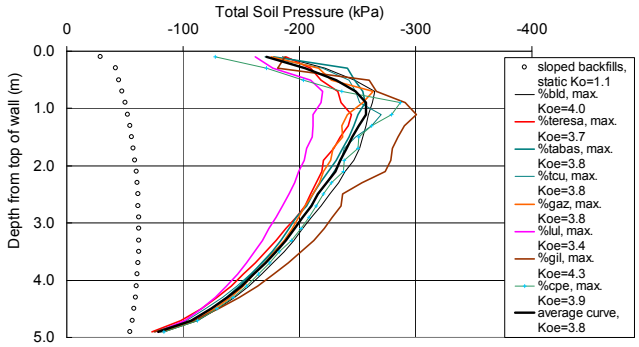

Fig. 17. Maximum soil pressures on walls with 2H:1V sloped backfills (φ=40°) under 1/2475 ground motions

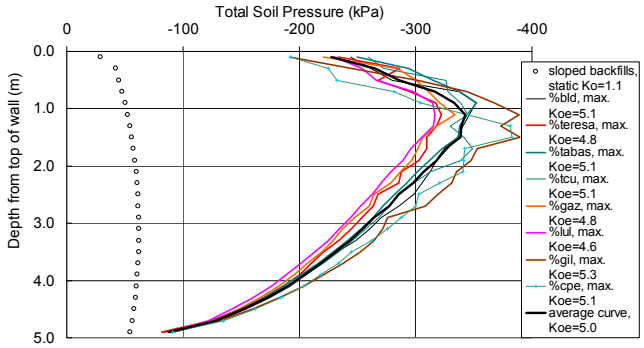

Fig. 18. Maximum soil pressures on walls with 2H:1V sloped backfills (φ=40°) under 1/10,000 ground motions

Table 2 Ground Displacements (m) at the Slope Crest as Estimated from VERSAT-2D Nonlinear Dynamic Analyses

	LOOSE SAND SLOPE, φ = 32°, K_g=868						DENSE SAND SLOPE, φ = 40°, K_g=1736					
	1/10,000		1/2475		1/475		1/10,000		1/2475		1/475	
	X-LATER	Y-DOWN	X-LATER	Y-DOWN	X-LATER	Y-DOWN	X-LATER	Y-DOWN	X-LATER	Y-DOWN	X-LATER	Y-DOWN
%bld	1.40	0.84	0.75	0.50	0.22	0.15	0.43	0.16	0.18	0.07	0.05	0.02
%teresa	1.53	1.00	0.91	0.62	0.30	0.23	0.54	0.29	0.17	0.10	0.03	0.01
%tabas	1.54	0.91	0.96	0.64	0.33	0.24	0.63	0.29	0.25	0.12	0.06	0.02
%tcu	3.70	2.28	2.12	1.48	1.00	0.79	1.20	0.47	0.50	0.20	0.10	0.04
%gaz	1.29	0.82	0.70	0.44	0.14	0.10	0.51	0.23	0.21	0.10	0.04	0.02
%lul	1.72	1.02	0.97	0.65	0.36	0.25	0.53	0.24	0.16	0.07	0.03	0.01
%gil	1.46	1.13	0.88	0.70	0.27	0.21	0.42	0.20	0.19	0.08	0.04	0.02
%cpe	2.52	1.58	1.58	1.03	0.52	0.38	1.03	0.40	0.40	0.15	0.06	0.02
Average	1.90	1.20	1.11	0.76	0.39	0.29	0.66	0.29	0.26	0.11	0.05	0.02

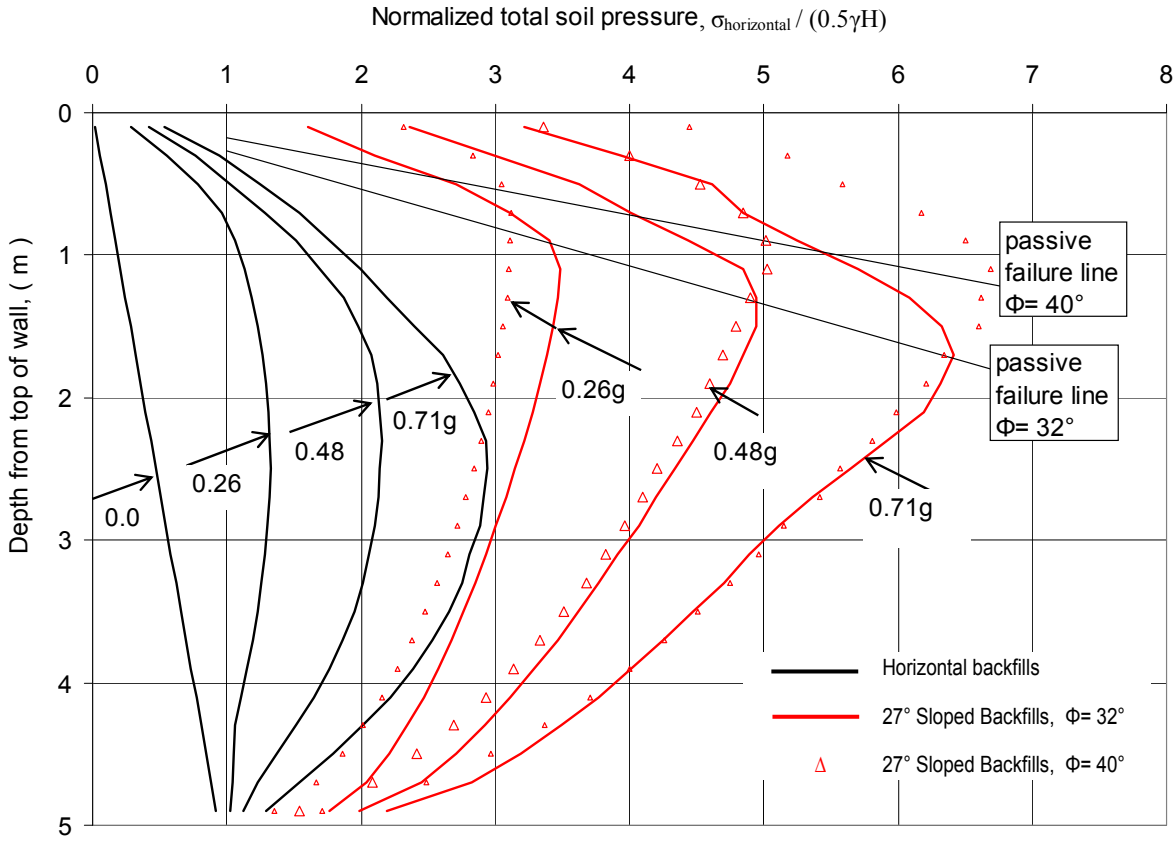

Fig. 19. Normalized soil pressure diagram from VERSAT-2D nonlinear analyses of a 5 m high wall with horizontal and 27º sloped backfills

SUMMARY

Seismic soil pressures on rigid walls retaining 2H:1V (27°) sloped backfills have been computed using a total of eight acceleration time histories recorded in past large earthquakes. These records were selected and linearly scaled to three levels of ground motions with a nominal PGA of 0.26g, 0.48g and 0.71g. Nonlinear time-history analyses were conducted using the computer program VERSAT-2D which uses a hyperbolic stress – strain model to simulate the hysteresis response of soil under cyclic loads. Soil pressure diagrams are shown in Fig. 19 for horizontal backfills (φ=32°), and for sloped backfills with loose sand (φ=32°) and dense sand (φ=40°) under the three levels of ground motions.

A soil pressure coefficient, K_{0E}, has been introduced to represent the total static and seismic pressures on a rigid (or non-yielding) wall. It is found that K_{0E} varies from 1.1, 1.7 to 2.2 for horizontal backfills under ground motions of 0.26g, 0.48g and 0.71g, respectively. K_{0E} (average for loose sand backfill and dense sand backfill) increases to 2.7, 3.8 and 4.9 for the 27° sloped backfills under the same three levels of ground motions, respectively.

The point of thrust is at about 0.47H above the base of wall for horizontal backfills, but for sloped backfills it increases to approximately 0.53H for loose sand and 0.55H for dense sand.

It should be noted that the purpose of this study is to illustrate a method of analysis, not to produce design charts on seismic pressures. Thus, it is recommended that site specific analyses be performed to determine seismic soil pressures for design of rigid walls.

REFERENCES

Bommer, J.J. and A.B. Acevedo [2004]. "The Use of Real Earthquake Accelerograms as Input to Dynamic Analysis", Journal of Earthquake Engineering, Vol. 8, Special issue 1, pp. 43-91.

Finn, W.D.L, K.W. Lee and G.R. Martin [1977]. "An Effective Stress Model for Liquefaction", ASCE Journal of Geotechnical Engineering, Vol. 103, pp. 517-533.

Adams, J. and G. Atkinson [2003]. "Development of Seismic Hazard Maps for the Proposed 2005 Edition of the National Building Code of Canada", Canadian Journal of Civil Engineering, Vol. 30, pp. 255-271.

Wood, J. H. [1973]. "Earthquake-induced Soil pressures on Structures", Ph.D thesis, the California Institute of Technology, Pasadena, California, USA

Wu, G. and S. Chan [2002]. "Design of the Russ Baker Way Overpass on Liquefiable Sand - Vancouver Airport Connector - Sea Island, Richmond, BC", Proceedings of the 6th International Conference on Short and Medium Span Bridges, Vancouver, pp. 579-586.

Wu, G. and W.D.L. Finn [1999]. "Seismic Lateral Pressures for Design of Rigid Walls", Canadian Geotechnical Journal, Vol. 36, pp. 509-522.

Wu, G. [2001]. "Earthquake Induced Deformation Analyses of the Upper San Fernando Dam under the 1971 San Fernando Earthquake", Canadian Geotechnical Journal, Vol. 38, pp. 1-15.

Wu, G., T. Fitzell and D. Lister [2006]. "Impacts of Deep Soft Soils and Lightweight Fill Approach Embankments on the Seismic Design of the Hwy. 15 North Serpentine River Bridges, Surrey, B.C.", Proceedings of the 59th Canadian Geotechnical Conference, Vancouver, pp. 596-601.

Wutec Geotechnical International [2001]. "VERSAT-2D: A Computer Program for Static and Dynamic 2-Dimensional Finite Element Analysis of Continua", Vancouver, B.C., Canada.